Structure and Properties of Poly(butylene succinate) Filled with Lignin: A Case of Lignosulfonate

Ning Lin,[1] Dongkuan Fan,[1] Peter R. Chang,[2] Jiahui Yu,[3] Xiaochun Cheng,[4] Jin Huang[1,5,6]

[1]*College of Chemical Engineering, Wuhan University of Technology, Wuhan 430070, China*
[2]*Saskatoon Research Centre, Agriculture and Agri-Food Canada, 107 Science Place, Saskatoon S7N 0X2, Saskatchewan, Canada*
[3]*College of New Drug Innovation Research and Development, East China Normal University, Shanghai 200062, China*
[4]*Key Laboratory of Attapulgite Science and Applied Technology of Jiangsu Province, Department of Chemical Engineering, Huaiyin Institute of Technology, Huai'an 223003, China*
[5]*State Key Laboratory of Pulp and Paper Engineering, South China University of Technology, Guangzhou 510640, China*
[6]*Key Laboratory of Cellulose and Lignocellulosic Chemistry, Guangzhou Institute of Chemistry, Chinese Academy of Sciences, Guangzhou 510640, China*

Received 17 July 2009; accepted 18 November 2010
DOI 10.1002/app.33754
Published online 4 March 2011 in Wiley Online Library (wileyonlinelibrary.com).

ABSTRACT: A new kind of blend material was prepared by the incorporation of lignosulfonate calcium (LS), as the filler, into biodegradable poly(butylene succinate) (PBS), as the polymeric matrix, with the process of melt mixing and subsequent compression molding. The nucleation of LS improved the crystalline properties of the PBS component in the blends. Combined with the rigidity nature of the LS filler, the Young's modulus values of the blends were enhanced. Furthermore, the introduction of LS in this biodegradable polyester slightly increased the hydrophilicity of the blends, shown as higher values of water uptake at equilibrium; this might facilitate the biodegradation of hydrophobic polyesters. Consequently, this study opened one way of enhancing the rigidity and decreasing the cost of biodegradable PBS-based polymeric plastics. © 2011 Wiley Periodicals, Inc. J Appl Polym Sci 121: 1717–1724, 2011

Key words: blends; nucleation; phase separation

INTRODUCTION

The development of biodegradable polymeric materials has been of great interest in recent years because of its contributions toward the protection of environment. However, there is a lack of wide-scale application of these materials in the industry largely because of the high cost.[1] Recently, poly(butylene succinate) (PBS), originated from renewable resources, depending on its excellent processability in the field of textiles, multifilaments, monofilaments, nonwovens, flats, and split yarns,[2,3] has been extensively developed as green films, biodegradable fibers, vessels, dishware, and injection-molded products.[4–7] Biodegradable PBS polymer is a white, semicrystalline thermoplastic with melting temperatures (T_m's) similar to that of low-density polyethylene, glass-transition temperatures (T_g's) and tensile strength (σ_b) values between those of polyethylene and polypropylene, and a stiffness between those of low-density polyethylene and high-density polyethylene;[2,8] it is considered highly promising as a commercial commodity polymer. Furthermore, in contrast with other persistent polymeric plastics, the predominant advantage of PBS is its easy

Correspondence to: J. Huang (huangjin@iccas.ac.cn) or P. R. Chang (peter.chang@agr.gc.ca).

Contract grant sponsor: National Natural Science Foundation of China; contract grant number: 50843031.
Contract grant sponsor: Agricultural Bioproducts Innovation Program of Canada (via the Pulse Research Network).
Contract grant sponsor: Fundamental Research Funds for the Central Universities (Self-Determined and Innovative Research Funds of Wuhan University of Technology); contract grant number: 2010-II-022.
Contract grant sponsor: Key Laboratory of Cellulose and Lignocellulosic Chemistry (Guangzhou Institute of Chemistry, Chinese Academy of Sciences); contract grant number: LCLC-2010-10.
Contract grant sponsor: State Key Laboratory of Pulp and Paper Engineering (South China University of Technology); contract grant number: 200906.
Contract grant sponsor: Natural Science Foundation of Jiangsu Province; contract grant number: BK2008195.
Contract grant sponsor: Key Laboratory of Attapulgite Science and Applied Technology of Jiangsu Province; contract grant number: HPK201003.

biodegradability in soil and by enzymes.[9–11] The chemical structure of PBS is as follows:

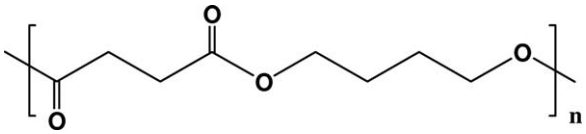

With the purpose of improving the performance and reducing the cost of PBS-based materials, cellulose acetate,[11] soy protein,[12] corn starch,[13,14] chitosan,[15] layered silicate,[3,16] organoclay,[17] attapulgite,[18] carbon nanotubes,[19] poly(lactic acid),[20] and poly (ethylene oxide)[21] have been introduced to modify the PBS plastics.

Lignin is a renewable, abundant, nontoxic, readily available, and low-cost resource, which shows a great potential as a filler for the development of fully biodegradable materials.[22,23] The positive factors of lignin as a modified component in the polymer matrix are as follows: it decreases the cost of the blends, it has good compatibility with natural and synthetic polymers because of the interaction between numerous functional groups of lignin and the polymer matrix, and it is an environmentally friendly filler in biodegradable, green blends. To this point, lignin has been incorporated as the reinforcing filler into all sorts of aliphatic polyesters,[24,25] such as polycaprolactone[26] and poly(L-lactic acid),[27] and has served to increase the modulus and/or improve the thermal properties. Consequently, the strategy of blending with lignin is a promising attempt to enhance the rigidity and lower the cost of the thermoplastic polymeric matrix. In this study, lignosulfonate calcium (LS), a water-soluble polydisperse polyelectrolyte with high rigidity, was selected as a natural filler to improve the performance of a PBS-based material. Because of its easy availability, low cost, and many kinds of active groups,[28,29] the introduction of LS as the filler into the PBS matrix was expected to enhance the rigidity and improve the crystalline and thermal behavior of the blends. Particularly, the high content of LS in the blends (the maximum content reached was 50 wt %) could sharply reduce the cost of PBS-based plastics and expand its application in many fields. The cost of PBS plastics would be 5 to 40% lower, according to the price in China. In this study, the structure and crystalline characters of PBS/LS blends containing different contents of LS were characterized by Fourier transform infrared (FTIR) spectroscopy, X-ray diffraction (XRD) and differential scanning calorimetry (DSC). The fractured morphologies of the blends were observed by scanning electron microscopy (SEM). At last, the mechanical properties of the PBS/LS blends were investigated by tensile testing, and the water absorption of the blends was measured to evaluate the hydroscopic properties. Moreover, the degree of miscibility and microphase separation between the fillers and matrix in the blends are discussed, and the role of the LS phase was further realized.

EXPERIMENTAL

Materials

Commercial PBS was purchased from Anqing Hexing Chemical Co., Ltd. (Anhui, China); its weight-average molecular weight (M_w) and relative density were 1.29×10^5 Da and 1.26, respectively. LS was donated by the Key Laboratory of Cellulose and Lignocellulosics Chemistry at Guangzhou Institute of Chemistry (Chinese Academy of Sciences, China), and its M_w was 2.66×10^4 Da, whereas the polydispersity (M_w/number-average molecular weight) was 2.98. All of the reagents are dehydrated *in vacuo* at 40°C for 12 h before use.

Melt mixing of PBS and LS

The blending of PBS and LS with various compositions was carried out in the internal mixer (Changzhou Suyan Science and Technology Co., Anhui, China). In the first instance, two mixing rotors of the machine were preheated to 110°C, and as-received PBS was kneaded into mixing trough with the rotating speed of 78 rpm. When the existent PBS intenerated because of the close temperature to its T_m (approximate to 115°C[14]), a suitable amount of LS was directly added to the kneaded PBS. With a rising temperature of 130°C and the same rotating speed as in initial conditions, the PBS matrix and LS filler were mixed for 10 min until macroscopic homogeneity was achieved. Subsequently, PBS/LS mixtures were prepared with different LS contents of 5, 10, 20, 30, 40, and 50 wt %. Finally, in comparison with the properties and performances of the blends, neat PBS was also banburied under the same conditions listed previously.

Compression molding of the PBS/LS blends

The PBS/LS melting blends were compression-molded with a 769YP-24B hot press (Keqi High Technology Co., Tianjin, China) as sheets at 120°C under a pressure of 20 MPa for 5 min and then air-cooled to about 25°C for a half-hour before the pressure for demolding was released. The dimensions of the obtained blend sheets with a thickness of about 0.2 mm were about 70×70 mm^2. The blends with different LS contents exhibited colors from light yellow to reddish brown, in contrast with the lily white

of the neat PBS sheet. According to the different contents of LS in the blends, the resultant blend sheets were coded as PBS/LS-5, PBS/LS-10, PBS/LS-20, PBS/LS-30, PBS/LS-40, and PBS/LS-50, respectively, in which the Arabic numerals represent the theoretical LS content of the PBS/LS blends. In addition, neat PBS sheets were also prepared according to the previous process without the addition of LS and were coded as PBS-F.

Characterization

FTIR spectroscopy of the PBS/LS blends were recorded on an FTIR 5700 spectrometer (Nicolet, Madison, WI). The sheets were scanned in the range 4000–700 cm^{-1} with Smart OMNT reflect accessories (Nicolet, Madison, WI).

XRD measurements were performed on a D/max-2500 X-ray diffractometer (Rigaku Denki, Tokyo, Japan) with Cu Kα_1 radiation ($\lambda = 0.154$ nm) in the range of $2\theta = 3$–60° with a fixed time mode with a step interval of 0.02°.

SEM observation was carried out on a Hitachi X-650 scanning electron microscope (Hitachi, Tokyo,-Japan). The sheets were frozen in liquid nitrogen and then snapped immediately. The fracture surfaces of the sheets were sputtered with gold and then observed and photo-graphed.

DSC analysis was performed on a DSC-Q200 instrument (TA Instruments, New Castle, DE) under a nitrogen atmosphere at a heating or cooling rate of 20°C/min. The sheets were scanned in the range of −70 to 150°C after a pretreatment (heating from 20 to 100°C and then cooling to −70°C) for eliminating the thermal history. The LS powder was scanned in the range of −70 to 250°C after the same pretreatment.

The mechanical parameters, including σ_b, elongation at break (ε_b), and Young's modulus (E), of all the sheets were measured on a CMT6503 universal testing machine (SANS, Shenzhen, China) with a tensile rate of 10 mm/min according to ISO527-3:1995(E). The testing sheets were cut as quadrate strips with a width of 10 mm, and the distance between testing marks was 40 mm. The testing strips were kept at a humidity of 35% for 7 days before measurement. The mean value of three replicates of each sheet was taken.

The water uptake of the blend sheets at a relative humidity (RH) of 98% was also studied. The specimens used were rectangular specimens with dimensions of 30 × 10 × about 0.20 mm^3. After the samples were weighed [initial weight (M_0)], the specimens were conditioned at room temperature in a desiccator containing a saturated $CuSO_4$ aqueous solution (RH of 98%). After a specific interval (t), the specimens were taken out and reweighed (M_t). The testing time was prolonged up to the invariant weight, that is, an equilibrium value. We calculated the water uptake value of the specimens by dividing the gain in weight ($M_t - M_0$) by M_0.[30] The average value of three replicates of each sample was taken.

RESULTS AND DISCUSSION

Mechanical properties of the PBS/LS blends

Figure 1 shows the effects of the LS content on the mechanical parameters of the PBS/LS blends, including σ_b, ε_b, and E. With an increase of the LS content from 0 to 50 wt %, the E values of the blends sharply increased from 596.16 to 1292.47 MPa; this indicated an enhancement of the rigidity of the blend materials. The improvement of E for all the blends was mainly attributed to the remarkable effects of incorporating the rigid LS fillers. However, it was pitiful that the increase of E depended upon the expense of the strength and elongation; namely, σ_b and ε_b gradually decreased with increasing LS content. Notably, the loading level of LS in the PBS matrix could reach 50 wt %, where the high loading level of LS could greatly lower the cost for meeting the requirements of applications. At this time, the resultant PBS/LS-50 showed the maximum E and values of 17.75 MPa for σ_b and 3.64% for ε_b. Furthermore, with regard to the decrease of σ_b, the main factor was lower elongation. When the blend sheets were broken in the tensile test, the stress could not be fully transferred to the rigid LS filler and crystalline PBS domain.

Crystalline character of the PBS/LS blends

The XRD patterns of the PBS/LS blends, neat PBS-F sheet, and the LS powder are shown in Figure 2. The semicrystalline character of PBS, that is, two sharp diffraction peaks located at 19.84 and 22.92° of 2θ, and two weak diffraction peaks located at 21.16 and 29.40° of 2θ, were observed in the patterns of the PBS-F and PBS/LS sheets. Meanwhile, with increasing LS content, the corresponding decrease in the PBS composition in the blends resulted in a gradual attenuation in the intensities of these peaks. On the other hand, the LS powder showed a broad and ambiguous diffraction pattern, namely, a predominant range of peaks centered around 20–25° of 2θ. This indicated that the LS mainly existed in an amorphous state. The LS as a filler usually plays a role of nucleation, which would improve the crystallinity of the PBS component in the blends. As a result, the diffraction characters of the PBS-based blends should have been more remarkable in theory. As shown in Figure 2, in the XRD patterns, the decrease in the peak intensities of the blends was

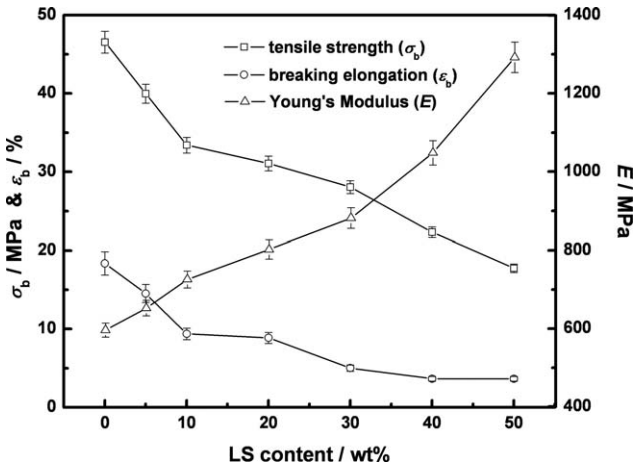

Figure 1 Effects of the LS contents on σ_b, ε_b, and E of the PBS/LS blends.

mainly attributed to the presence and even the increasing content of the amorphous LS component.

As is well known, the transformations of the crystalline domain and amorphous region are a kind of essential change in the blend that nearly affects the microphase separation structure and, at last, determines the mechanical properties of the materials. Figure 3 shows the attenuated total reflection (ATR)–FTIR spectra of the blends containing various LS contents and the neat PBS-F reference. In this

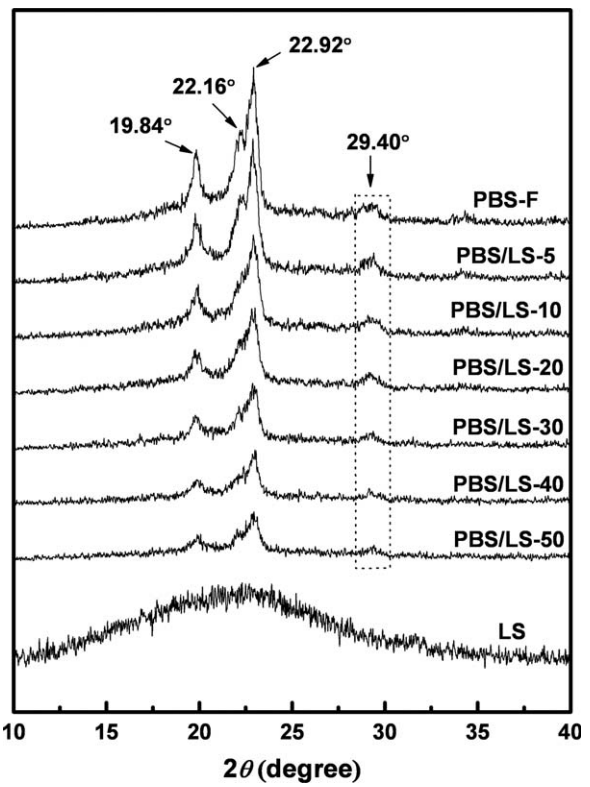

Figure 2 XRD patterns of the PBS/LS blends with various LS contents and LS powder and neat PBS-F as references.

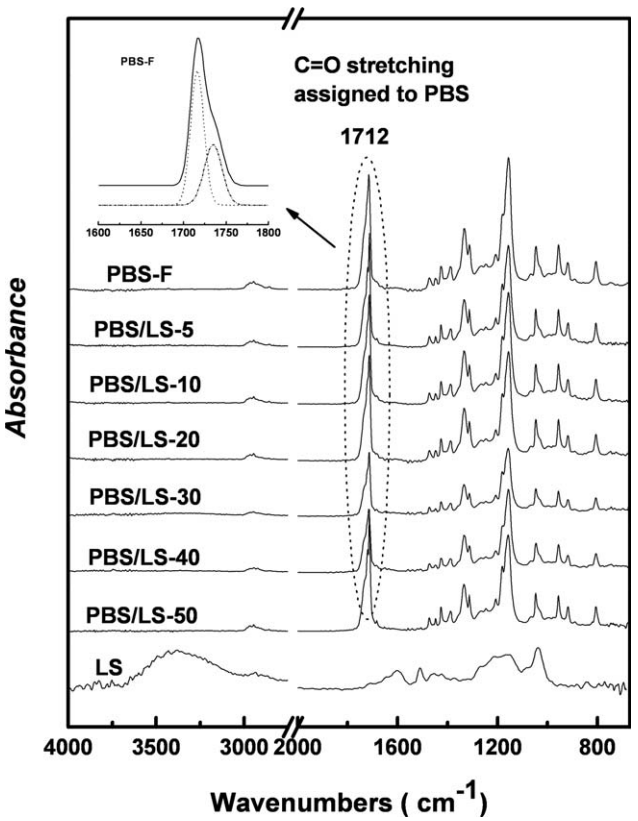

Figure 3 Full ATR–FTIR spectra of the PBS/LS blends with various lignin contents and neat PBS-F and curve-fitted FTIR spectra of neat PBS-F in the range 1600–1800 cm^{-1}: (—) experimental curve, (···) —C=O in the crystalline domain, and (---) —C=O in the amorphous region.

case, the —C=O groups consisted of a main peak located at about 1714 cm^{-1} assigned to the PBS component, and there were some slightly shifts (1712 cm^{-1}) and changes in the relative intensities of blends in this region; these were attributed to the crystalline–amorphous transformation of the PBS component in the blends. As a result, the spectra from 1600 to 1800 cm^{-1} of all of the PBS/LS blends and PBS-F (as shown in the small legend of Fig. 3) were divided into two peaks by curve fitting, that is, peak I located at 1714–1717 cm^{-1} and peak II located at 1734–1736 cm^{-1}. The former was the —C=O stretching in the crystalline domain for the PBS matrix, which was constructed by the ordered and arranged PBS chains, whereas the latter was the —C=O stretching of random arranged PBS chains in the amorphous PBS region. Table I summarizes the detailed location and fraction of peaks I and II for all of the PBS/LS blends and neat PBS-F sheet. With increasing LS contents, the percentage of —C=O in the crystalline domain versus that in the amorphous region changed regularly. Compared with that of the neat PBS-F (62.51%), the percentage of —C=O in the crystalline domain of all of the PBS/LS blends was augmented and increased from about 63.25% (PBS/

TABLE I
Location and Fraction of Curve-Fitting Peaks for the —C=O Absorption in the FTIR Spectra of PBS/LS Blends with Various LS Contents

	—C=O band			
	Peak I[a]		Peak II[b]	
Sample	Location (cm^{-1})	Fraction (%)	Location (cm^{-1})	Fraction (%)
PBS	1716.17	62.51	1734.81	37.49
PBS/LS-5	1714.99	63.25	1734.22	36.75
PBS/LS-10	1715.38	65.10	1734.81	34.90
PBS/LS-20	1715.78	66.36	1735.20	33.64
PBS/LS-30	1715.58	64.87	1735.60	35.13
PBS/LS-40	1715.97	63.40	1734.81	36.60
PBS/LS-50	1714.80	64.17	1735.60	35.83

[a] —C=O in the crystalline domain.
[b] —C=O in the amorphous region.

LS-5) to about 66.36% (PBS/LS-20) and decreased to about 64% when the LS content was higher than 30 wt %. This indicated that the introduction of LS improved the crystallinity of the PBS component in the blends. Herein, the improvement in the crystalline properties of the PBS component might have been due to the nucleation role of the LS filler.

Thermal properties of the PBS/LS blends

To clarify the difference in the thermal behaviors, DSC was used to further understand the interactions and crystalline properties in the PBS/LS blends via observation of the variances of the domain-scale glass transition and the melting transition of the crystalline domains assigned to the PBS component, respectively. Figure 4 shows the DSC thermograms of the neat PBS-F and PBS/LS blends, whereas Table II summarizes the glass-transition temperature at the midpoint ($T_{g,\mathrm{mid}}$), heat-capacity increment (ΔC_p), T_m, and heat enthalpy of the blends ($\Delta H_{m,\mathrm{PBS/LS}}$) and the heat-capacity increment and heat enthalpy assigned to the PBS component ($\Delta C_{p,\mathrm{PBS}}$ and $\Delta H_{m,\mathrm{PBS}}$, respectively). $T_{g,\mathrm{mid}}$ of LS powder was about 178.4°C, which was in agreement with the reported values of T_g of LS, which varied from 127 to 193°C. The interactions between the LS filler and the PBS matrix affected the free motion of the PBS segments; meanwhile, these interactions induced the crystallinity of the PBS component under the nucleation of LS filler. All of the interactions and the crystalline–amorphous transformation of the PBS component were reflected by the T_g and T_m values of the blends. With increasing LS content from 0 to 10 wt %, the values of $T_{g,\mathrm{mid}}$ of the blends increased slightly; this indicated that the rigid LS filler inhibited the motion of the PBS segments. However, when the LS content was higher than 20 wt %, the $T_{g,\mathrm{mid}}$ values of the blends were lower than that of the neat PBS. This resulted from the microphase separation between the aggregated LS and PBS matrix, although the improved PBS crystalline augmented the inhibition of the motion of the PBS segments. Correspondingly, the values of T_m first increased from 115.0 to 115.3°C (PBS/LS-10) and then decreased to 109.7°C with the increase of LS content from 20 to 50 wt %. Furthermore, compared with the $\Delta H_{m,\mathrm{PBS}}$ value of neat PBS-F at 89.3 J/g, all of the blends showed dramatically higher $\Delta H_{m,\mathrm{PBS}}$ values. This proved the enhancement of the crystallization of

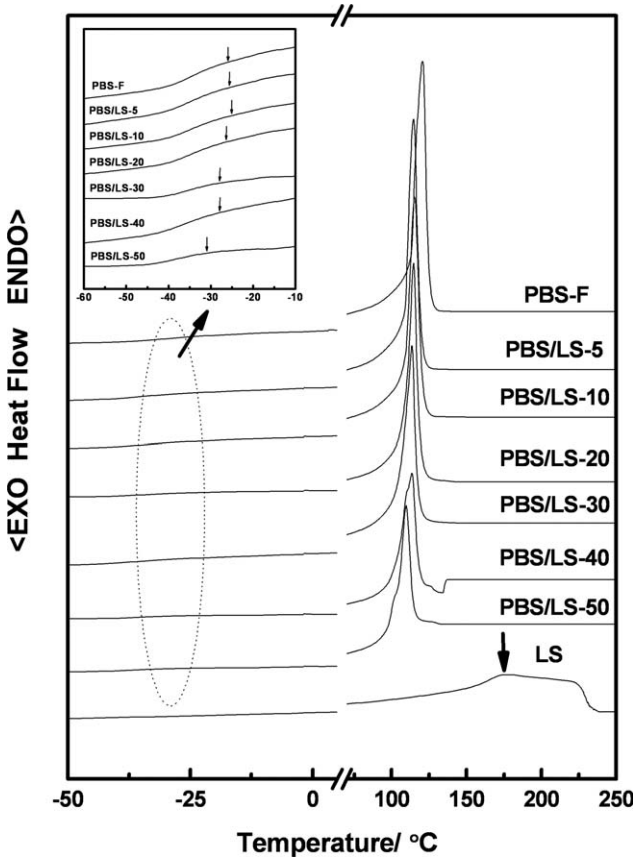

Figure 4 DSC thermograms of PBS/LS blends with various LS contents and neat PBS-F and LS powder as references.

TABLE II
$T_{g,\mathrm{mid}}$, T_m, ΔC_p, and ΔH_m Values from DSC Thermograms

Sample	$T_{g,\mathrm{mid,PBS}}$ (°C)	$\Delta C_{p,\mathrm{PBS/LS}}$ [J/(g °C)]	$\Delta C_{p,\mathrm{PBS}}$ [J/(g °C)]	$T_{m,\mathrm{PBS}}$ (°C)	$\Delta H_{m,\mathrm{PBS/LS}}$ (J/g)	$\Delta H_{m,\mathrm{PBS}}$ (J/g)
PBS	−25.9	—	0.18	115.0	—	89.3
PBS/LS-5	−25.6	0.17	0.18[a]	114.6	84.9	89.4[b]
PBS/LS-10	−25.0	0.15	0.17[a]	115.3	90.1	100.1[b]
PBS/LS-20	−26.4	0.086	0.11[a]	114.7	85.1	106.4[b]
PBS/LS-30	−27.9	0.086	0.12[a]	113.5	67.2	96.0[b]
PBS/LS-40	−27.7	0.077	0.13[a]	113.6	54.3	90.5[b]
PBS/LS-50	−30.9	0.073	0.15[a]	109.7	47.3	94.6[b]

[a] $\Delta C_{\mathrm{p,PBS}} = \Delta C_{\mathrm{p,PBS\&LS}}/(1 - x)$, where x is the weight percentage of LS.
[b] $\Delta H_{m,\mathrm{PBS}} = \Delta H_{m,\mathrm{PBS/LS}}/(1 - x)$.

the PBS component, in agreement with the curve-fitted ATR–FTIR spectra in Figure 4 and the resultant data in Table I. Interestingly, the $\Delta H_{m,\mathrm{PBS}}$ values of the blends increased from 89.3 to 106.4 J/g when the LS content increased from 0 to 20 wt % and then decreased with the addition of more LS. This indicated that a higher LS content resulted in the self-aggregation of LS and inhibited the ordered arrangement and, hence, induced the microphase separation between the LS filler and the PBS matrix to facilitate free motion of the PBS chains. At this time, the $\Delta H_{m,\mathrm{PBS}}$ values decreased. On the other hand, the $\Delta H_{m,\mathrm{PBS/LS}}$ values of the blends decreased sharply from 89.3 to 47.3 J/g (with the addition of 50 wt % LS) with increasing LS contents; this was mainly attributed to the large decrease in the PBS composition. This was in agreement with the attenuation of crystalline diffraction in the XRD pattern of Figure 2. On the whole, the addition of LS filler improved the crystallinity of the PBS component because of the nucleation of LS phase, whereas the higher content of LS filler (>20 wt %) gradually augmented the microphase separation between the LS filler and the PBS matrix. The increase in the ordering of the PBS chains influenced by the LS content, proved by DSC and FTIR analysis, might also facilitate the enhancement of Young's modulus.

Fractured morphologies of the PBS/LS blends

SEM images of the fracture surfaces of the neat PBS-F and PBS/LS blends are shown in Figure 5. Except for the PBS/LS-5 and PBS/LS-10 blends with lower LS loading levels, the fractured morphologies of the PBS/LS blends were distinctly different from the curly grain of the fractured surface of the PBS-F sheet. The PBS/LS-5 and PBS/LS-10 blends showed analogical striation on the fractured surface; this indicated some extent degree of miscibility between the LS filler and PBS matrix and the relatively uniform dispersion of LS in the PBS matrix. Compared with neat PBS-F, the changes in fractured morphology of the PBS/LS-20 blend indicated that the presence of microphase separation between the LS filler and PBS matrix. Nevertheless, it was difficult to distinguish the dispersion of individual filler at such contents of LS filler. However, when the LS content was increased to 30 wt %, many small LS phases dispersed in the PBS matrix were observed distinctly [as shown in the arrow of Fig. 5(e)]. With the continuous increase in LS content (40 and 50 wt %), the serious self-aggregation of the LS fillers and the induced microphase separation between the LS filler and PBS matrix caused a coarser fractured morphology with some holes and separated layers.

Water uptake of the PBS/LS blends

The diffusion of water is strongly influenced by the microstructure of blends, which affects gas, water, and solute permeability.[14] The water uptake up to the equilibrium of blend sheets and the PBS-F sheet under an RH of 98% is plotted as a function of time (t) in Figure 6. Two well-separated zones were observed, zone I ($t < 100$ h), for rapidly increasing water uptake, and zone II ($t > 100$ h), for approaching the equilibrium of water uptake. The neat PBS-F sheet had a water uptake at equilibrium of about 2%. In this case, when the testing specimens were permeated by the evaporated water, the low motion freedom of the PBS chains and the dense crystalline region restricted the permeation of water vapor. All of blend sheets showed a higher water uptake at equilibrium, and the values increased up to a maximum of about 20% when 40 wt % LS was added. This suggested that the introduction of LS, a kind of hydrophilic filler, improved the water absorption of the PBS-based blends. When the hydrophilic LS filler dispersed and/or self-aggregated in the blends, the decrease in the PBS crystalline domains in the blends and the hydrophilic properties of LS facilitated the absorption of water vapor.

Role of the LS filler in the PBS-based composites

Attributed to the homogeneous dispersion of the lower loading level of LS, the PBS/LS-5 and PBS/LS-

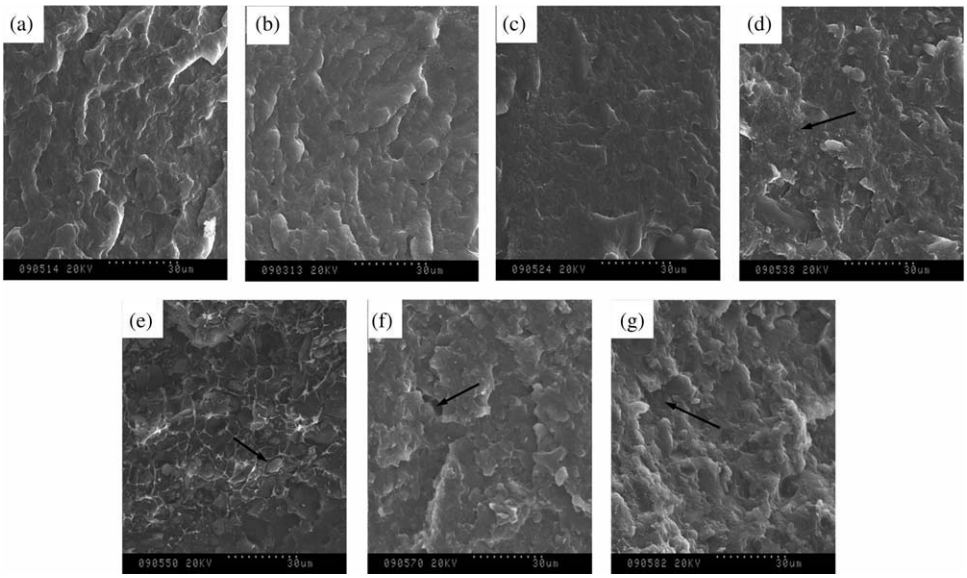

Figure 5 SEM images of the fractured surfaces of (a) neat PBS-F (as a reference) and the (b) PBS/LS-5, (c) PBS/LS-10, (d) PBS/LS-20, (e) PBS/LS-30, (f) PBS/LS-40, and (g) PBS/LS-50 blends.

10 blends exhibited some extent degree of miscibility between LS filler and PBS matrix. Hence, the nucleation of LS filler enhanced the crystallinity of the PBS component and, thus, produced an increase in $\Delta H_{m,\mathrm{PBS}}$. The reinforcement effect, originating from the LS rigidity and the improved crystallinity of the PBS component proved by the results of XRD, FTIR, and DSC, produced higher E values in the blends. The decrease in the σ_b at break was mainly relevant to the decrease of elongation. Compared with the neat PBS-F, the performances of this blend (PBS/LS-20) were the turning point; for instance, the $\Delta H_{m,\mathrm{PBS}}$ values of the blends reached the maximum of 106.4 J/g, and the water uptake at equilibrium of the PBS/LS-20 blend increased greatly in contrast to PBS/LS-10. This resulted from the occurrence of microphase separation between the LS filler and the PBS matrix due to the self-aggregation of superfluous LS fillers. At this time, the strength and elongation of the blends decreased sharply. With an increase in the LS content, the obvious self-aggregation of the LS filler and the reduction of the PBS component led to a decrease in the crystallinity of the blends, which showed the decreased $\Delta H_{m,\mathrm{PBS}}$ values. However, the rigidity of LS and its aggregates still supported the increase in E.

CONCLUSIONS

LS was incorporated into the PBS matrix to produce new blend materials with a higher rigidity and low cost. Compared with the neat PBS material, the blends filled with LS showed enhanced E at the expense of elongation and strength. Meanwhile, the introduction of LS increased the hydrophilicity of the resultant blend material, and hence, the blend exhibited higher values of water uptake at equilibrium. XRD patterns proved that PBS was the semicrystalline polymer and there was crystalline PBS component in the PBS-based blends. Furthermore, the results of the curve-fitted —C=O stretching peaks and $\Delta H_{m,\mathrm{PBS}}$ show that the crystallinity of the PBS component in the blends was improved; this was attributed to the nucleation function of the LS filler. However, when the LS content was higher than 20 wt %, $\Delta H_{m,\mathrm{PBS}}$ in the blends was lower than that of the neat PBS; this indicated microphase separation between the LS filler and the PBS matrix. Consequently, the introduction of LS as a filler not

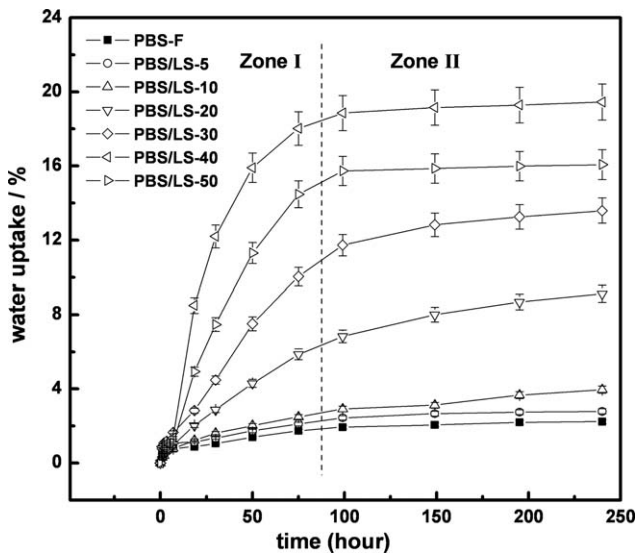

Figure 6 Water uptake with 98% RH for PBS/LS blends with various LS contents and neat PBS-F as a reference.

only remarkably increased the rigidity but also sharply lowered the cost of the thermoplastic PBS-based materials. This is expected to extend the practical application of biodegradable PBS plastics.

References

1. Sen, A.; Bhattacharya, M. Polymer 2000, 41, 9177.
2. Fujimaki, T. Polym Degrad Stab 1998, 59, 209.
3. Ray, S. S.; Okamoto, K.; Okamoto, M. Macromolecules 2003, 36, 2355.
4. Lenz, R. W. Adv Polym Sci 1993, 107, 1.
5. Ishii, M.; Okazaki, M.; Shibasaki, Y.; Ueda, M.; Teranishi, T. Biomacromolecules 2001, 2, 1267.
6. Shirahama, H.; Kawaguchi, Y.; Aludin, M. S.; Yasuda, H. J Appl Polym Sci 2001, 80, 340.
7. Huang, J.; Zhang, L.; Chen, F. J Appl Polym Sci 2003, 88, 3284.
8. Li, Y. D.; Zeng, J. B.; Wang, X. L.; Yang, K. K.; Wang, Y. Z. Biomacromolecules 2008, 9, 3157.
9. Honda, N.; Taniguchi, I.; Miyamoto, M.; Kimura, Y. Macromol Biosci 2003, 3, 189.
10. Lee, S. H.; Ohkita, T.; Kimura, A. Polym Prepr 2003, 52, 1091.
11. Uesaka, T.; Nakane, K.; Maeda, S.; Ogihara, T.; Ogata, N. Polymer 2000, 41, 8449.
12. Ohkita, T.; Lee, S. H. J Appl Polym Sci 2005, 97, 1107.
13. Sen, A.; Bhattacharya, M.; Stelson, K. A.; Voller, V. R. Mater Sci Eng 2002, 338, 60.
14. Coutinho, D. C.; Pashkuleva, I. H.; Alves, C. M.; Marques, A. P.; Neves, N. M.; Reis, R. L. Biomacromolecules 2008, 9, 1139.
15. He, Y.; Zhu, B.; Kai, W.; Inoue, Y. Macromolecules 2004, 37, 8050.
16. Glasser, W. G. Forest Prod J 1981, 31, 24.
17. Shih, Y. F.; Wang, T. Y.; Jeng, R. J.; Wu, J. Y.; Teng, C. C. J Polym Environ 2007, 15, 151.
18. Chen, C. H. J Phys Chem Sol 2008, 69, 1411.
19. Song, L.; Qiu, Z. Polym Degrad Stab 2009, 94, 632.
20. Harada, M.; Ohya, T.; Iida, K.; Hayashi, H.; Hirano, K.; Fukuda, H. J Appl Polym Sci 2007, 106, 1813.
21. Lu, J.; Qiu, Z.; Yang, W. Macromol Mater Eng 2008, 293, 930.
22. Kringstad, K. In Future Source of Organic Raw Material: Chemrawn I; St.-Pierre, L. E.; Brown, G. R., Eds.; Pergamon: New York, 1980; p 627.
23. Klason, C.; Kubat, J. Plast Rubber Proc Appl 1986, 6, 17.
24. Li, Y.; Sarkanen, S. Macromolecules 2002, 35, 9707.
25. Li, Y.; Sarkanen, S. Macromolecules 2005, 38, 2296.
26. Nitz, H.; Semke, H.; Landers, R.; Mülhaupt, R. J Appl Polym Sci 2001, 81, 1972.
27. Li, J.; Inoue, Y. Polym Int 2003, 52, 949.
28. Cui, G.; Xia, W.; Chen, G.; Wei, M.; Huang, J. J Appl Polym Sci 2007, 106, 4257.
29. Rydholm, S. A. Pulping Processes; Interscience: New York, 1985.
30. Anglès, M. N.; Dufresne, A. Macromolecules 2000, 33, 8344.